Journal of Engineering Research and Application Volume 1, December 2022,
http://dx.doi.org/10.55953/JERA.2022.2104 pp. 24-32

Prediction of Compressive Strength of Geopolymer Concrete using Artificial Neural Network

Kamal Upreti[1], Manvendra Verma[2*]

[1] Associate Professor, Department of Computer Science and Engineering, Dr Akhilesh Das Gupta Institute of Technology and Management, New Delhi, India.

kamalupreti1989@gmail.com

[2] Assistant Professor, Department of Civil Engineering, Dr Akhilesh Das Gupta Institute of Technology and Management, New Delhi, India.

mv075415@gmail.com

Abstract: - Geopolymer concrete could be an alternative to ordinary Portland cement concrete. It is sustainable, eco-friendly, durable, and economic concrete. Machine learning methods could an alternatives to determines strength without destruction tests conduction of the mix samples. In this study, to analyse the experimental investigation and prediction of compressive strength using artificial neural network. In experimental analysis, M2 mix got optimum point in the compressive strength among all mixes. ANN model is used to predict the compressive strength of geopolymer concrete. ANN model prediction has negligible errors. So, it can be stated that machine learning methods are capable to predicts the strength of concrete accurately.

Keywords: - Geopolymer concrete; machine learning; artificial neural network; mechanical strength

1. Introduction

After water, cement concrete is the second most plentiful substance used in the world, and it is the most widely used [1]. Cement is the most valuable ingredient of concrete since it serves as a binding constituent in the concrete mix, making it extremely durable. Because the production of one tonne of Portland cement generates about one tonne of CO_2, it pollutes the environment at a very high level, causing global warming [2]. By substituting industrial solid waste such as fly ash, GGBFS, rice husk ash, and metakaolin for the entirety of the cement content, GPC directly minimises the pollution caused by the scenario [3]–[6]. These industrial solid waste materials include high levels of alumina (Al_2O_3) and silica (SiO_2) content [7]–[12]. NaOH and Na_2SiO_3 are present in the industrial solid waste that has been activated by the alkaline solution and function as an adhesive material in the concrete. Davidovits used the term "geopolymer" in 1978 to refer to the natural rock polymers that form as a result of the chemistry of the rocks themselves. Known as geopolymer, an inorganic alumina-silicate polymer, it is made up of a large proportion of silicon and aluminium elements derived from topographical starting or outcome materials combined [13]–[16]. The synthetic arrangement of geopolymer components is similar to that of zeolite. However, reveal a three-dimensional microstructure. During the coordinated operation, the Si and Al ions consolidate to form a structural hindrance that is artificially and virtually identical to the structural hindrance that connects the ordinary rocks [17].

Because of the large amount of silica in bituminous and anthracite coals, they produce low-calcium fly ash, which possesses pozzolanic qualities due to its low calcium content. Sub-bituminous or lignite coals, on the other hand, produce a substantial amount of fly ash with a high calcium concentration, which may be used as a pozzolanic or cementitious material (it has less silica and alumina, but more significant CaO content) [18]. According to ASTM 618-08, there are two types of fly ash remains class F, which is short in CaO and has a substance of less than 10% and is found in bituminous coals; and class H, which is long in CaO and has a material of more than 10% and is found in lignite coals. Class C coals are high in CaO and contain more than 10% substance, and they are delivered by lignite and sub-bituminous coal, respectively. According to ASTM C989, regular class F fly ash contains 4.3 percent CaO, whereas other class C fly ash contains 27.4 percent CaO. The use of fly ash in mixed designs takes advantage of the outcomes of concrete hydration, such as calcium hydroxide, which is often a source of weakness in normal bond cement and transforms them into denser, more grounded C-S-H mixtures through the pozzolanic reaction. Because of

ISSN 2583-3987

the heat generated during the hydration process, the pozzolanic reaction of fly ash begins (ACI 1995). The presence of fly ash response items in concrete that has been properly alleviated reduces the solid porousness to water and aggressive synthetic chemicals. Stable gains qualities from properly proportioned fly ash cement blends that would otherwise be impossible to achieve using only Portland bond alone. Because they make use of naturally hazardous material, these mixes are more durable, practical, dependable, and environmentally friendly. The various parameter affects the mechanical strength of geopolymer concrete [19]–[30]

The creation of models for estimating the strength characteristics of concrete is a continuous process that is carried out to eliminate the need for excessive repetition of tests and waste of resources. Popular methods for modelling concrete qualities include best-fit curves (which are based on regression analysis), which are widely used in the construction industry [31]. As a result of the nonlinearity of concrete, the models produced via regression analysis may not accurately represent the underlying nature of the concrete. Furthermore, regression models may be unable to detect a substantial difference in the effects of component elements in concrete [32].

In the subject of civil engineering, modern modelling approaches such as the artificial neural network (ANN) and genetic programming have been discovered to be useful. Experimental validation of these methodologies is carried out to model responses based on the included input parameters and to verify the output models. Parichatprecha and Nimityongskul demonstrate that artificial neural networks (ANNs) are capable of producing appropriate outputs in a variety of settings, including data categorization, prediction, optimization, and forecasting (2009). GEP and ANN are used in construction applications to forecast the strength of concrete, the performance of bituminous mixes, and the durability of concrete. GEP and ANN have also been detected in other products such as recycled aggregate concrete, asphaltic concrete, and blast furnace slag. On the basis of publicly accessible data from the open literature, GEP and ANN exhibit a significant ability to solve scientific and engineering issues. The use of GEP and ANN to anticipate the characteristics of geopolymer self-compacting concrete (GSCC) has not been extensively investigated despite the documented examples of modelling geopolymer concrete parameters. This paper includes models for forecasting the strength features of GSCC that have been built using GEP and ANN approaches. According to expectations, geopolymer field applications should be well represented by these models.

2.1 Experimental Program

2.1.1 Materials

For this experiment, sodium hydroxide was acquired from the Central Drug House (P) Ltd. in New Delhi, India. In the material sample, sodium hydroxide crystallises as white deliquescent flakes with a purity level of 96.0 percent at the lowest end of the scale. It was acquired from the Central Drug House (P) Ltd. in New Delhi, 110002 and is known as sodium silicate solution (water glass) (India). Sodium silicate exists in compact, tacky, slightly cloudy liquid form, with a minimum assay of Na_2O titrimetric of 10.0 percent and SiO_2, gravimetric of 25.5-28.5 percent of the sample solution. The isolation of molten slag with the aid of high-pressure water jets results in the formation of GGBFS. Because of the separation of the molten slag, crystallisation is prevented, and the end products are discovered as glassy and granular aggregates. Because of the variety of uses, the final product is crushed, pulverised, and sorted for each application. The GGBFS utilised in the project was sourced from the Bhilai Steel Plant in Durg, Chhattisgarh, India, according to the manufacturer. Table 1 lists the chemical compositions of the sample materials and exhibits a porous, undefined form due to the presence of porous, undefined-shaped particles of GGBFS. During the electricity generating process, fly ash is formed in thermal power plants by the burning of coal in the boilers. In India, fly ash is collected from the Gurunanak Dev thermal power plant in Bhatinda, Punjab. According to the ASTM C618-33512 categorization system, fly ash is classified as Class C. Table 1 lists the chemical compositions of the sample materials and the porous spherical particles of fly ash in a porous spherical shape. In the mix design of the experiments, m-sand or stone dust that was readily accessible in the area was employed as a fine aggregate. Generally speaking, stone dust is a well-graded medium sand kind found in zone II. This material has 1.21 percent water absorption, 2.62 percent specific gravity, 6% silt content, and a bulk density of 1610 kg/m^3 [33]–[40]. The materials were subjected to an X-ray diffractometer (XRD) examination at the Delhi Technological University's central facility laboratory. The sample was subjected to XRF, SEM, and EDS examinations at the Nano laboratory of Jamia Millia Islamia, New Delhi. In the concrete laboratory of the civil engineering department of Delhi Technological University, Delhi, all destructive and non-destructive testing on the GPC specimens was carried out.

Table 1 Mineral composition of GGBFS and Flyash

Characteristics	SiO_2	Al_2O_3	CaO	Fe_2O_3	MgO	SO_3	LOI
Flyash (%)	**45.8**	**21.4**	**13.7**	**12.6**	**1.3**	**1.9**	**.1**
GGBFS (%)	**34.52**	**20.66**	**32.43**	**.57**	**10.09**	**.77**	**.3**

2.1.2 Synthesis

It was necessary to combine NaOH flakes with the Na2SiO3 solution to create an activator solution with a weight-to-volume ratio of 1:1 by weight. The hot liquid alkaline solution was let to cool for 20-24 hours to adjust to the ambient temperature. GPC specimens are mixed with four different ratios of fly ash and GGBFS in the alkaline solution synthesised in this research: fly ash/(fly ash + GGBFS) being.25,.50,.75, and 1.0, respectively, with the alkaline solution synthesised in this investigation. The mass ratio of the alkaline solution (NaOH and Na2SiO3) to the dry mix (fly ash and GGBFS) was 0.4 in this experiment. Fine aggregate and coarse aggregate were completely mixed with fly ash, GGBFS, fine aggregate, and coarse aggregate until a homogeneous blend was generated for the samples mould. After that, the alkaline solution was combined with the dry concrete mix to make concrete in the pan mix. Samples mould in the shape of a cube, a cylinder, and a beam segment, all in accordance with IS code. Following the demould samples, the moulded samples were dried at room temperature before being dried in the oven with hot air. Table 2 is a list of all of the GPC's design combinations.

Table 2 Mix Proportion

Mix Designs	Flyash to GGBFS Ratio	Cement (kg/m^3)	Fly ash (kg/m^3)	GGBFS (kg/m^3)	Coarse Aggregate (kg/m^3)	Fine Aggregate (kg/m^3)	NaOH Solution (kg/m^3)	Sodium Silicate (kg/m^3)	Super Plasticizer (kg/m^3)	Extra Water (kg/m^3)
M1	**100/0**	**-**	**405**	**-**	**1269**	**683**	**81.0 (13M)**	**81.0**	**-**	**81**
M2	**75/25**	**-**	**303.75**	**101.25**	**1269**	**683**	**81.0 (13M)**	**81.0**	**-**	**81**
M3	**50/50**	**-**	**202.5**	**202.5**	**1269**	**683**	**81.0 (13M)**	**81.0**	**-**	**81**
M4	**25/75**	**-**	**101.25**	**303.75**	**1269**	**683**	**81.0 (13M)**	**81.0**	**-**	**81**

2.1.3 Test Setup

To check for density differences between cubical, cylindrical, and prism-shaped GPC mix samples, use various sized moulds and varied shapes of GPC mix samples according to the IS code and weight after the demoulding and at the time of testing. Make a concrete mix mould with dimensions of 150 mm x 150 mm x 150 mm to determine the compressive strength of the mix design. Furthermore, the test was performed on a universal testing machine under axial force. Make cylindrical samples in 150mm diameter moulds with a length of 300mm to test the splitting tensile strength of the concrete mix design specimen in a laboratory setting. In the universal testing machine, a transverse force is applied to the cylinder to examine the splitting tensile strength of the GPC cylinder specimen. Construct the beam samples in moulds with dimensions of 100mm in width, height, and length, and 500mm in length and width to test the flexural tensile strength of the specimens designed using the GPC mix design. Produce cylindrical specimens in moulds with a maximum diameter of 150 mm and a maximum length of 300 mm to evaluate the modulus of elasticity and poisons ratio of the concrete mix design sample. In a universal testing machine, an axial load was applied to the cylinder to examine the vertical and horizontal strain of a Geopolymer concrete cylinder specimen to determine the modulus of elasticity and poisons ratio of the Geopolymer concrete cylinder specimen.

The term "rebound hammer" refers to equipment that tests the strength of a hardened sample of geopolymer concrete without causing damage to the specimens of a GPC mix. Both kinds of sample cube and cylinder tests are used to determine the strength of the mixed samples.

The UPV test is a non-destructive test that is used to determine how long the UPV will travel through concrete. When calculating the UPV in a material, the travelling time of the ultrasonic pulse is taken into consideration. The UPV provides clarity on the quality or strength of the concrete being tested. The exceptional quality and great strength of the concrete are shown by the UPV. In the UPV test setup, there are two transducers, an ultrasonic pulse generator and an amplifier that measures the time it takes for the sound to travel between the transducers to be detected.

3. Modelling

The idea of artificial neural networks is applicable to a wide range of issues in science and engineering, and it is becoming more popular. It is often used in the development of predictive statistical models for complex processes that are essentially nonlinear in nature, such as biological systems. The use of ANN allows for the simulation of a wide range of complicated system behaviour. The ANN functioning is considerably more similar to that of a regular human brain, having components that are referred to as neuron components. It is also possible to compare the notion of ANN to the way a computer runs, as in the phrase "garbage in, garbage out," since it employs input factors to replicate the system process in order to determine the output variables. In other words, the construction of an ANN model necessitates the inclusion of input and output components, the latter of which is completely controlled by the former. This concept is systematic in that the neurons are connected together and each connection has its own weight, which makes up the ANN principle. As a result, the solution to the model is obtained by multiplying the weight by the number of transmitted signals in the network. The input layer, hidden layers, and output layer are the three layers that make up a standard ANN network design. The input and output layers are established before data training, however, the hidden layer is found by trial and error after data training. Figure 4 is a representation of a common ANN architectural model. The model comprises input factors (x1, x2, x3, x4---- xn) and weights (W1, W2, W3, W4---- Wn), with weights (W1, W2, W3, W4---- Wn) for each factor. Singular value or sum function (sigmoid) processing is the ultimate processing method, and it has the final impact on the output (s). A broad description of the analogy is provided in Eq. 1, output, where Wn denotes weight and Xn denotes input, and b is the bias of the analogy. It has been shown in research that the ANN approach is capable of predicting meaningful replies, regardless of whether the data being processed is strewn with mistakes or even incomplete [63,64]. The ANN approach is composed of three steps, which are learning, training, and model performance testing. Learning is the first of these activities. To ensure that output variables are properly predicted during the training stage, weights and biases in the network (supervised or unsupervised) are adjusted to ensure that the output variables are reliably predicted. The supervised training method makes use of already completed experimental data for model construction, while the unsupervised training method does not make use of real-world input and output data.

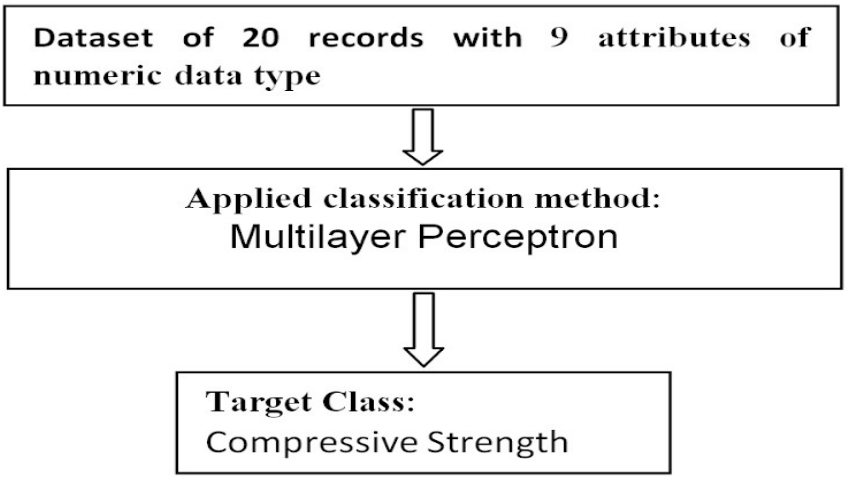

Fig. 1 Flow chart of ANN or multilayer perception model

It is possible that the network will respond to the input without changing the overall network design during the testing stage. At every step of the ANN creation process, a number of trial-and-error procedures are carried out before the optimum network can be chosen. Following the completion of the trial-and-error process, Alshihri discovered that it could be prolonged in order to generate a large number of networks, after which the process could be stopped and tested at various stages of the learning process Using alternative sets of random weights, reanalyse the network and continue the procedure until the desired result is achieved. Finally, a suitable ANN architecture is defined as the model that produces the least mean square error (MSE) between the anticipated output and the actual outputs recorded in the training data. The performance of the ANN model was evaluated via the use of the MATLAB programme. It was decided to utilise error backpropagation, which employs the straining and recall algorithms, for the model construction process. In the opinion of Lee, this technique has the potential to tackle issues involving several variables (multidimensional). As shown in Table 3, the input and output datasets that were employed in this work for model construction are given. The data was trained using a feed-forward backpropagation model based on the Levenberg–Marquardt (LM)multilayer approach, which is accessible in the MATLAB programming environment. ANN models were developed using a data set of 105 data samples generated from this investigation and other relevant studies,

which included the data samples from this study. A total of three parts were created from the input data; seventy percent of the data was utilised during the learning phase, and fifteen percent each was used during the testing and validation stages. The data were normalised by default in MATLAB, as opposed to manual division with maximum values, which was done manually. The method was performed many times using trial and error until the most appropriate model was found that met the MSE criterion.

4. Results and Discussion

4.1 Fresh and Hardened properties of concrete

For compressive strength testing, all of the mix designs samples were cured by oven curing at 800C for 24 hours, and the samples were tested after seven days, fourteen days, twenty-eight days, forty-two days, and fifty-six days in UTM. M4 has the highest compressive strength of all cured samples. The dose of GGBFS is about 25% of the fly ash in the mix design, which results in an immediate increase in the strength of the mix. However, if you exceed the 25% dose of GGBFS, the mix designs become a little less powerful. The highest average compressive strength of the 100/0, 50/50, and 25/75 binding ratio mixes was 18.2 N/mm2, 21.8 N/mm2, and 20.3 N/mm2 after 56 days, respectively. When tested at 56 days, the average compressive strength of the oven-cured samples of GPC in which the 75/25 binding ratio mix obtained the highest average compressive strength was 32.9 N/mm2. The GPC specimens had reached around 95% strength after 28 days, but they had grown significantly weaker.

All of the mixed design samples were cured by oven curing at 800C for 24 hours, and the samples were tested in the UTM for splitting tensile strength after seven days, fourteen days, twenty-eight days, forty-two days, and fifty-six days. The 75/25 fly ash/GGBFS ratio mix design samples have the highest splitting tensile strength of all cured samples. The substitution of GGBFS with fly ash results in a modest drop in the splitting tensile strength of the mix design samples, following the rise in the splitting tensile strength caused by the addition of fly ash to the mix design samples at a rate of 25% by weight. The average splitting tensile strength of oven-cured samples of GPC is shown with the 75/25 fly ash/GGBFS ratio mix having the highest average splitting tensile strength of 4.8 N/mm2 at 56 days, and with the 100/0, 50/50, and 25/75 fly ash/GGBFS ratio mixes having the lowest average splitting tensile strength of 3.2 N/mm2, 4.6 N/mm2, and 4.2 N/ After 28 days, the GPC specimens have gained around 95 percent of their original strength; after that, they have acquired just a little bit of strength.

All of the mix design samples were cured by the oven-curing methods at a temperature of 80 °C for 24 hours, and the samples were tested for flexural strength at seven days, fourteen days, twenty-eight days, forty-two days, and fifty-six days using a flexural testing machine. All cured samples with the 75/25 fly ash/GGBFS ratio mix design have the highest average flexural tensile strength of all cured samples. When GGBFS is mixed with fly ash at a 25 percent by weight concentration, the samples' flexural tensile strength immediately increases. The substitution of GGBFS with fly ash, even after the increase, results in a minor drop in the flexural tensile strength of the mix designs samples after the increase. The flexural strength of oven-cured samples of GPC is shown with the 75/25 fly ash/GGBFS ratio mix obtaining the highest average flexural tensile strength of 5.3 N/mm2 at 56 days, while the 100/0, 50/50, and 25/75 fly ash/GGBFS ratio mixes obtained the highest average flexural tensile strength of 3.6 MPa, 4.9 MPa, and 4.6 MPa at 56 days. Approximately 95 percent of the GPC samples' strength was obtained after 28 days, after which they developed significantly less strength.

All of the mixed design samples were oven cured for 24 hours at a temperature of 800 °C, and the samples were tested by rebound hammer test under the non-destructive test of concrete specimens at seven days, fourteen days, twenty-eight days, forty-two days, and fifty-six days. 75/25 fly ash/GGBFS ratio mix design samples have the highest average rebound hammer strength. At a rate of 25 percent by weight, adding GGBFS and fly ash to design mix samples at a rate of 25 percent by weight results in an immediate increase in the rebound strength of the samples, but following the increase, replacing GGBFS with fly ash causes a small drop in the rebound strength of the design mix specimens. The highest average rebound hammer strength was 35 N/mm2 for the 75/25 fly ash/GGBFS ratio mix. The highest average rebound hammer strength for the 100/0, 50/50, and 25/75 fly ash/GGBFS ratio mixes is 28.9 N/mm2, 33.8 N/mm2, and 32.7 N/mm2 for After 28 days, the GPC specimens have gained around 95 percent of their original strength; after that, they have acquired just a little bit of strength. The rebound hammer test strength was a little stronger than the destructive compressive strength of the same mix design specimens that were tested.

The ultrasonic pulse velocity test is a non-destructive method of testing the material under consideration. The UPV test equipment is comprised of two transducers, one of which is used to produce an ultrasonic pulse wave into the material and the other which is used to receive the wave transmitted through the material during the testing process. A 150mm GPC sample cube is used to detect the velocity of the UPV wave as it travels through it. The natural frequency

of 55kHz is used to send information using cube samples. Both transducers maintain their positions at the opposite ends of the cube in order to achieve the smallest possible displacement between the transducers. The cube's surface should be clean in order to transmit the UPV wave as effectively as possible. The UPV tests on the samples were performed at intervals of seven days, fourteen days, twenty-eight days, forty-two days, and fifty-six days after the casting of the specimens. The ratio of 75/25 fly ash to GGBFS produced the highest UPV of all of the mix designs. The UPV graphs also indicate tendencies that are comparable to those seen in another non-destructive rebound hammer test. Among all the mix designs tested in both cured conditions, the ratio of 100/00 fly ash to GGBFS produced the lowest UPV of any of them. The UPV of the GPC specimens grows with the number of days that have passed since the casting. It has a direct impact on the overall strength of the GPC specimens. The amount of UPV in the mix designs changes depending on the amount of fly ash-GGBS in the mix designs. When the GGBFS dose is increased from 0 percent of the binder to up to 25 percent of the binder, the UPV rises instantly. When the dose of GGBFS is increased by more than 25%, the UPV begins to decrease somewhat as well. The maximum ultrasonic pulse velocity of the oven-cured specimens is 4.226 km/sec. After the 28-day testing, the UPV of the GPC specimens rises by a very small proportion.

4.2 ANN Modelling Results

The ANN model predicts the compressive strength of the geopolymer concrete based on their constituents content present in the mix design. Initially, to create a model based on the actual data that are found through the experimental investigationin the laboratory. This process has different phases like data collection, data testing, and data training. Fig. 2 shows the different phases to develop ANN model. Fig. 3 shows the layers of the ANN model which includes thee input layer, hiden layer, and output layer. In this validation, used the two crossfold validation to found the errors between actual data and predicted data of compressive strength. Table 3 shows the different errors found between the predicted data and actual data of compressive strength. The result coefficient, MAE, RMSE, RAE, and RRSE were found during the validation of the results. It shows the errors are found very less in percentages. It can be called as negligible error.

Table 3 Detail of various error

Correlation coefficient (R^2)	0.982
Mean absolute error (MAE)	0.5303
Root mean squared error (RMSE)	0.6863
Relative absolute error (RAE)	17.5477 %
Root relative squared error (RRSE)	18.7538 %

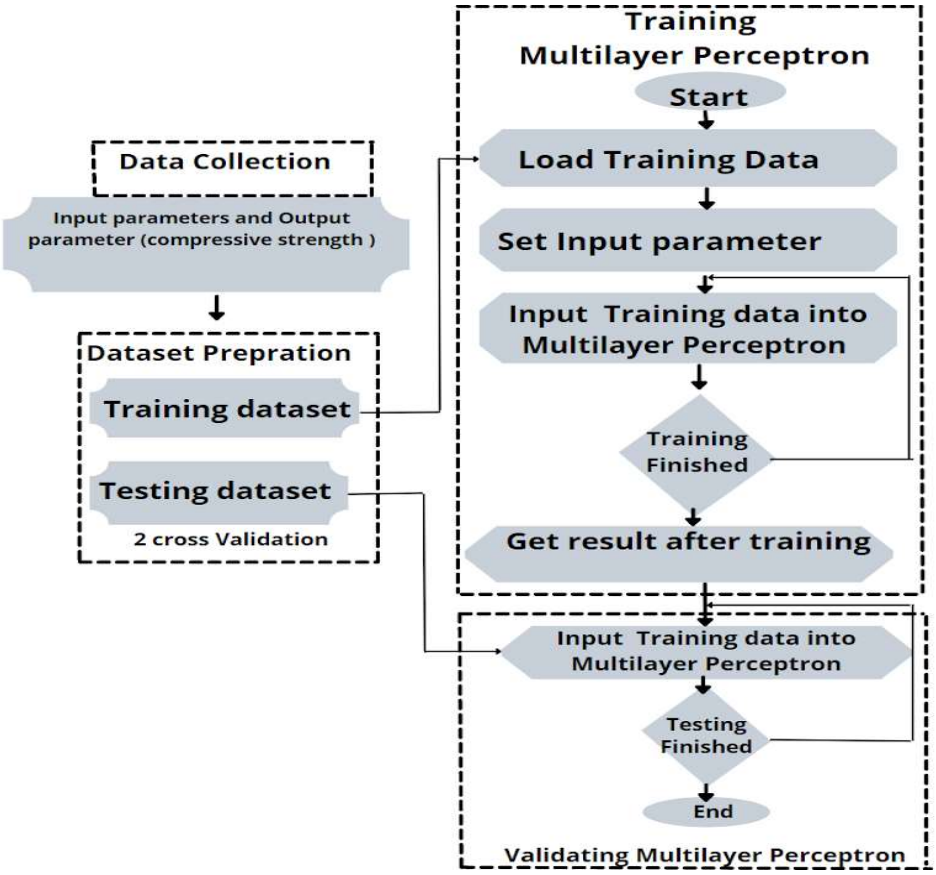

Fig. 2 Different phases of ANN model to develop and validate

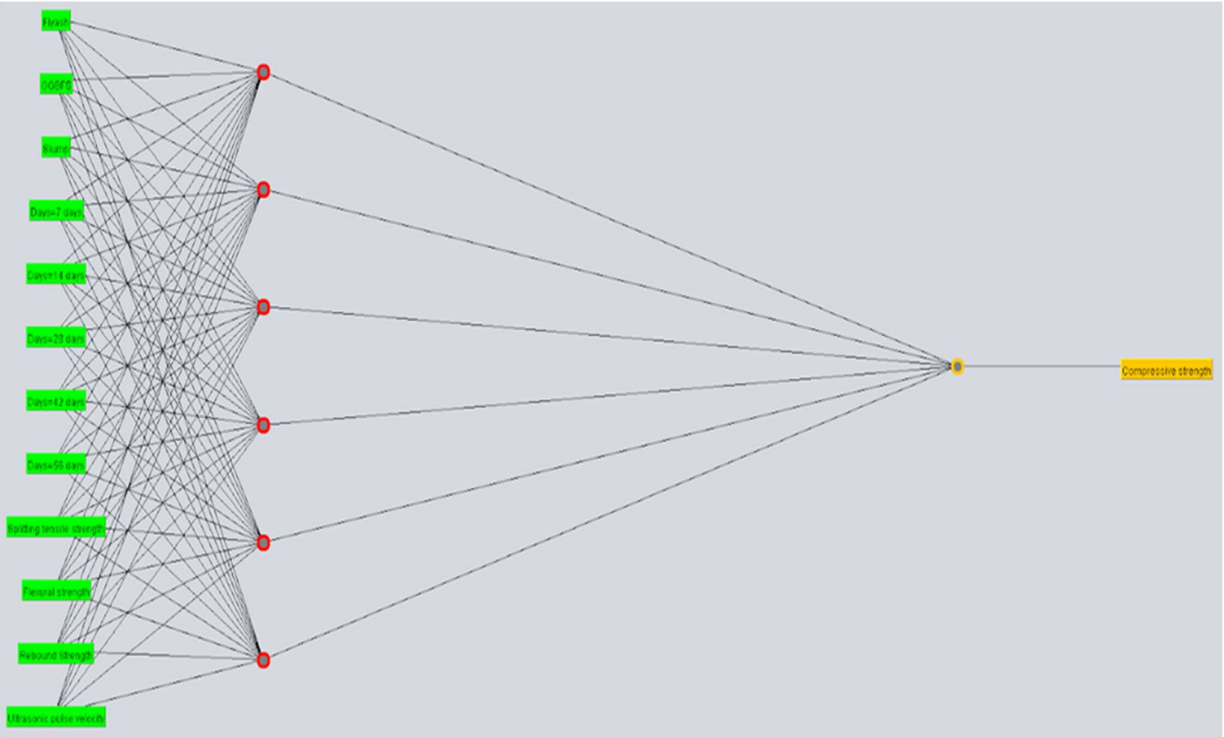

Fig. 3 Layers of ANN model

5. Conclusion

After the experimental investigation and prediction using ANN models. The following conclusion are as:

- In experimental analysis, M2 mix got optimum point in the compressive strength among all mixes.
- ANN model is used to predict the compressive strength of geopolymer concrete. ANN model prediction has negligible errors.

References

[1] B. Sabir, S. Wild, and J. Bai, "Metakaolin and calcined clays as pozzolans for concrete: A review," *Cem. Concr. Compos.*, vol. 23, no. 6, pp. 441–454, 2001.

[2] J. G. J. Olivier, K. M. Schure, and J. A. H. W. Peters, "TRENDS IN GLOBAL CO2 AND TOTAL GREENHOUSE GAS EMISSIONS Summary of the 2017 report," no. 2983, 2017.

[3] J. Davidovits, "30 Years of Successes and Failures in Geopolymer Applications. Market Trends and Potential Breakthroughs.," in *Geopolymer 2002 Conference, October 28-29, 2002, Melbourne, Australia*, 2002, pp. 1–16.

[4] J. Davidovits and S. Quentin, "Geopolymers Inorganic polymeric new materials," *J. ofThamalAnalysis*, vol. 37, pp. 1633–1656, 1991.

[5] J. Davidovits, "Geopolymers and Geopolymeric Materials," *J. Therm. Anal.*, vol. 35, pp. 429–441, 1989.

[6] Joseph Davidovits, *Geopolymer Chemistry & Applications*. 2015.

[7] P. K. Mehta and P. J. M. Monteiro, *Concrete Microstructure, Properties, and Materials*, vol. 4. 2014.

[8] K. tuo Wang, Y. He, X. ling Song, and X. min Cui, "Effects of the metakaolin-based geopolymer on high-temperature performances of geopolymer/PVC composite materials," *Appl. Clay Sci.*, vol. 114, pp. 586–592, 2015.

[9] Y. Wang, T. Zheng, X. Zheng, Y. Liu, J. Darkwa, and G. Zhou, "Thermo-mechanical and moisture absorption properties of fly ash-based lightweight geopolymer concrete reinforced by polypropylene fibers," *Constr. Build. Mater.*, vol. 251, p. 118960, 2020.

[10] N. Li, C. Shi, Z. Zhang, H. Wang, and Y. Liu, "A review on mixture design methods for geopolymer concrete," *Compos. Part B Eng.*, vol. 178, no. April, p. 107490, 2019.

[11] Y. J. Zhang, S. Li, Y. C. Wang, and D. L. Xu, "Microstructural and strength evolutions of geopolymer composite reinforced by resin exposed to elevated temperature," *J. Non. Cryst. Solids*, vol. 358, no. 3, pp. 620–624, 2012.

[12] P. He, D. Jia, T. Lin, M. Wang, and Y. Zhou, "Effects of high-temperature heat treatment on the mechanical properties of unidirectional carbon fiber reinforced geopolymer composites," *Ceram. Int.*, vol. 36, no. 4, pp. 1447–1453, 2010.

[13] H. Xu and J. S. J. Van Deventer, "Geopolymerisation of multiple minerals," *Miner. Eng.*, vol. 15, pp. 1131–1139, 2002.

[14] H. Su, J. Xu, and W. Ren, "Mechanical properties of geopolymer concrete exposed to dynamic compression under elevated temperatures," *Ceram. Int.*, vol. 42, pp. 3888–3898, 2016.

[15] F. Xu, X. Deng, C. Peng, J. Zhu, and J. Chen, "Mix design and flexural toughness of PVA fiber reinforced fly ash-geopolymer composites," *Constr. Build. Mater.*, vol. 150, pp. 179–189, 2017.

[16] X. Chen, S. Wu, and J. Zhou, "Influence of porosity on compressive and tensile strength of cement mortar," *Constr. Build. Mater.*, vol. 40, pp. 869–874, 2013.

[17] R. Haddad and I. Al-Qadi, "Characterization of Portland Cement Concrete Using," *Cem. Concr. Res.*, vol. 28, no. 10, pp. 1379–1391, 1998.

[18] I. Bhavan, "Indian Minerals Yearbook 2015 SLAG-IRON AND STEEL (ADVANCE RELEASE) GOVERNMENT OF INDIA MINISTRY OF MINES INDIAN BUREAU OF MINES," 2016.

[19] M. Verma and N. Dev, "Geopolymer concrete : A way of sustainable construction," *Int. J. Recent Res. Asp.*, vol. 5, no. 1, pp. 201–205, 2018.

[20] M. Verma and N. Dev, "Effect of ground granulated blast furnace slag and fly ash ratio and the curing

conditions on the mechanical properties of geopolymer concrete," *Struct. Concr.*, pp. 1–15, 2021.

[21] M. Verma and N. Dev, "Effect of SNF-Based Superplasticizer on Physical, Mechanical and Thermal Properties of the Geopolymer Concrete," *Silicon*, vol. 14, no. 3, pp. 965–975, 2021.

[22] M. Verma and N. Dev, "Effect of Liquid to Binder Ratio and Curing Temperature on the Engineering Properties of the Geopolymer Concrete," *Silicon*, vol. 14, no. 2022, pp. 1743–1757, 2022.

[23] M. Verma and M. Nigam, "Mechanical Behaviour of Self Compacting and Self Curing Concrete," *Int. J. Innov. Res. Sci. Eng. Technol.*, vol. 6, no. 7, pp. 14361–366, 2017.

[24] M. Verma, N. Dev, I. Rahman, M. Nigam, M. Ahmed, and J. Mallick, "Geopolymer Concrete : A Material for Sustainable Development in Indian Construction Industries," *Crystals*, vol. 12, no. 2022, p. 514, 2022.

[25] R. Kumar, M. Verma, and N. Dev, "Investigation on the Effect of Seawater Condition, Sulphate Attack, Acid Attack, Freezet-haw Condition, and Wetting–Drying on the Geopolymer Concrete," *Iran. J. Sci. Technol. Trans. Civ. Eng.*, pp. 1–31, 2021.

[26] M. Verma, "Experimental investigation on the properties of Geopolymer concrete after replacement of river sand with the M-sand," in *International e-Conference on Sustainable Development & Recent Trends in Civil Engineering*, 2022, vol. 46–54, no. January.

[27] R. Kumar, M. Verma, and N. Dev, "Investigation of fresh , mechanical , and impact resistance properties of rubberized concrete," in *International e-Conference on Sustainable Development & Recent Trends in Civil Engineering*, 2022, no. January, pp. 88–94.

[28] M. Verma and N. Dev, "Review on the effect of different parameters on behavior of Geopolymer Concrete," *Int. J. Innov. Res. Sci. Eng. Technol.*, vol. 6, no. 6, pp. 11276–281, 2017.

[29] A. Chouksey, M. Verma, N. Dev, I. Rahman, and K. Upreti, "An investigation on the effect of curing conditions on the mechanical and microstructural properties of the geopolymer concrete," *Mater. Res. Express*, vol. 9, no. 2022, p. 055003, 2022.

[30] M. Verma and N. Dev, "Sodium hydroxide effect on the mechanical properties of flyash-slag based geopolymer concrete," *Struct. Concr.*, vol. 22, no. S1, pp. E368–E379, 2021.

[31] P. O. Awoyera, "Nonlinear finite element analysis of steel fibre-reinforced concrete beam under static loading," *J. Eng. Sci. Technol.*, vol. 11, no. 12, pp. 1669–1677, 2016.

[32] A. Sadrmomtazi, J. Sobhani, and M. A. Mirgozar, "Modeling compressive strength of EPS lightweight concrete using regression, neural network and ANFIS," *Constr. Build. Mater.*, vol. 42, pp. 205–216, 2013.

[33] IS 2386 (Part VI), "Methods of test for aggregates for concrete Part VI Measuring mortar making properties of fine aggregate," *Bur. Indian Stand.*, vol. 2386, no. October 1963, 1997.

[34] IS 2386 (Part VII), "Methods of test for aggregates for concrete Part VII Alkali aggregate reactivity," *Bur. Indian Stand.*, 1997.

[35] IS 383 1970, "Specification for coarse and fine aggregates from natural sources for concrete," *Bur. Indian Stand.*, no. 1997, pp. 1–20, 1997.

[36] IS 2386 (PartV), "Methods of test for aggregates for concrete Part V Soundness," *Bur. Indian Stand.*, 1997.

[37] IS 2386 (Part II), "Methods of test for aggregates for concrete Part II Estimation of deleterious materials and organic impurties," *Bur. Indian Stand.*, vol. 2386, no. October 1963, 1998.

[38] IS 2386 (Part IV), "Methods of test for aggregates for concrete Part IV Mechanical Properties," *Bur. Indian Stand.*, vol. 2386, no. March 1964, 1997.

[39] IS 2386 (Part III), "Methods of test for aggregates for concrete Part III Specific gravity, density, voids, absorption and bulking," *Bur. Indian Stand.*, vol. 2386, no. October 1963, 1997.

[40] IS 2386 (Part I), "Methods of test for aggregates for concrete Part I Particle size and shape," *Bur. Indian Stand.*, vol. 2386, 1997.